Journal of Materials Chemistry C

PAPER

View Article Online
View Journal | View Issue

Cite this: J. Mater. Chem. C, 2015, 3, 1301

Synthesis and self-assembly of 5,5′-bis(phenylethynyl)-2,2′-bithiophene-based bolapolyphiles in triangular and square LC honeycombs†

Hongfei Gao,‡[a] Huifang Cheng,‡[a] Zonghan Yang,[ab] Marko Prehm,[c] Xiaohong Cheng*[a] and Carsten Tschierske*[c]

Received 17th October 2014
Accepted 20th November 2014

DOI: 10.1039/c4tc02347a

www.rsc.org/MaterialsC

A series of X-shaped 5,5′-bis(phenylethynyl)-2,2′-bithiophene-based bolaamphiphiles bearing two long lateral alkyl chains and two terminal glycerol groups has been synthesized by using Kumada and Sonogashira coupling reactions as key steps. The thermotropic liquid crystalline behavior of these compounds was investigated by POM, DSC and X-ray scattering. With elongation of the lateral alkyl chains two different kinds of liquid crystalline phases with honeycomb structures, $Col_{hex}\Delta/p6mm$, formed by (defective) triangular honeycomb cells, and $Col_{squ}/p4mm$ with square cells were observed for these compounds. UV and PL measurements indicate fluorescent properties making them potential candidates for application in fluorescence sensor devices.

1. Introduction

The preparation of well-defined nanostructures through ingenious molecular self-assembly is of current interest for numerous advanced technological applications.[1] Some examples include metal–organic frameworks (MOFs) and covalent organic frameworks (COFs) forming solid state structures with square or hexagonal channels that provide a permanent porosity for storage and catalysis applications.[2] Moreover, MOFs and COFs involving π-conjugated aromatic building blocks have attracted significant interest as candidates for semiconducting organic materials.[3] Remarkably, very similar polygonal honeycomb structures, with an even wider range of different cylinder shapes, ranging from triangular *via* square, pentagonal to hexagonal and beyond, were recently obtained in a fluid, liquid crystalline (LC) state,[4–8] which is a unique state of soft matter combining order and mobility on a molecular to macroscopic level.[6,9] The majority of these fluid honeycombs are formed by polyphilic rod-like molecules with flexible lateral chains whereby the chains fill the hollow space inside the honeycomb cells and contribute to the fluidity of the self-assembled overall superstructures.[10] Another source of their mobility arises from the dynamic character of the hydrogen bonding networks between the polar glycerol groups located at both ends of the rod-like and lipophilic cores, and which interconnect the aromatic rods to the network structures. Thus, the rigid and geometrically fixed metal coordination sites and covalent linkages in solid state MOFs and COFs, respectively, are replaced by dynamic hydrogen bonding networks located at the ends of these T-shaped[4,5] or X-shaped[11] bolapolyphilic LC molecules.[12] This leads to unique fluids with compartmented honeycomb structures, representing columnar LC phases with π-conjugated rod-like cores laying perpendicular to the column long axis and forming cell walls enclosing the channels filled by the lateral chains. This unique mode of soft self-assembly has been confirmed experimentally[5] and supported by simulation work.[13] Due to the dynamic character of these structures and the combination of order and mobility, they can be affected by external stimuli, producing supramolecular self-assembled systems for diverse applications. Moreover, as a result of the inherent mobility, transitions between honeycombs with distinct geometries can easily be achieved.[5,6] Among these, the transition between triangular and square honeycombs is of special interest, because the combination of both types of cells in a uniform structure could lead to periodic and quasiperiodic arrays that combine the triangular and square cylinders in distinct ratios.[5,6,13–16] Oligo(phenylene)s and oligo(phenylene ethynylene)s have predominately been used as rigid rod-like cores for the design of T-shaped and X-shaped bolapolyphiles.[4–6,11] In order to introduce functionality into these soft

[a]Key Laboratory of Medicinal Chemistry for Natural Resources, Yunnan University, Kunming 650091, P. R. China. E-mail: xhcheng@ynu.edu.cn; Fax: +86 871 5032905
[b]Faculty of Chemistry and Environmental Health, Dalian University of Technology, Dalian 116024, P.R. China
[c]Institute of Chemistry, Organic Chemistry, Martin-Luther University Halle-Wittenberg, Kurt Mothes Str. 2, 06120 Halle/Saale, Germany. E-mail: carsten.tschierske@chemie.uni-halle.de; Fax: +49 345 55 27346

† Electronic supplementary information (ESI) available. See DOI: 10.1039/c4tc02347a

‡ Both authors contributed equally to this work.

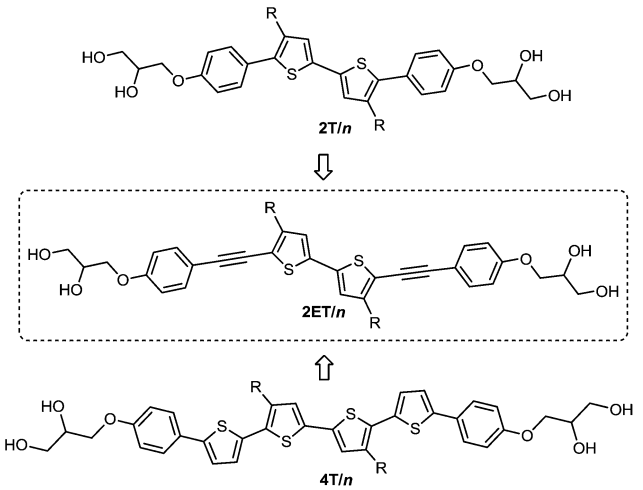

Scheme 1 Compounds **2ET/*n*** under investigation and the related previously reported dithiophene-based bolapolyphiles **2T/*n***[19] and tetrathiophene-based bolapolyphiles **4T/*n***.[20]

nanostructures for their use in potential applications, oligothiophene segments have been employed as rod-like building blocks.[17–21] Honeycomb-type columnar phases with triangular ($Col_{hex}\Delta/p6mm$), square ($Col_{squ}/p4mm$), and hexagonal cells ($Col_{hex\text{-}6}/p6mm$) have been found for these compounds based on bithiophene (**2T/*n***, Scheme 1),[18,19] tetrathiophene (**4T/*n***),[20] and hexathiophene cores[21] by varying the length and number of the lateral alkyl chains.

Besides these oligothiophenes, compounds involving additional ethynylene units are also attractive for providing electron conducting[22] and fluorescencent properties.[23] Herein, we report a new series of dithiophene based X-shaped bolapolyphiles **2ET/*n*** incorporating additional ethynylene units (**E**) in the rigid core, and compare them with the related compounds **2T/*n*** and **4T/*n*** without these ethynylene units (see Scheme 1). Such compounds can be considered as being intermediates between compounds **2T/*n*** and **4T/*n*** because they contain dithiophene units just like the **2T/*n*** series and have almost the same core length, just like the tetrathiophene-based bolapolyphiles **4T/*n***.

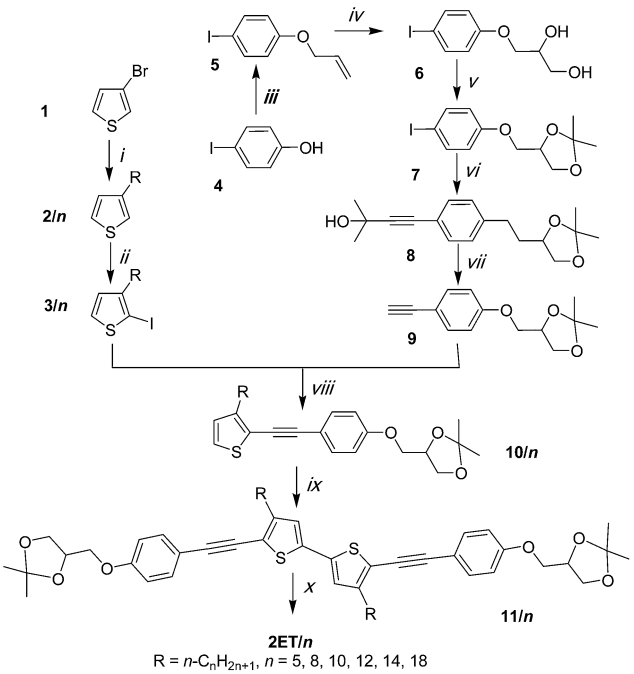

Scheme 2 Synthesis of compounds **2ET/*n***. Reagents and conditions: (i) $C_nH_{2n+1}MgBr$, $Ni(dppp)Cl_2$, THF, reflux, 15 h, 75–86%; (ii) NIS, CH_2Cl_2, CH_3COOH, RT, 2 h, 90–95%; (iii) 3-bromoprop-1-ene, K_2CO_3, CH_3CN, reflux, 15 h, 92%; (iv) OsO_4, NMMNO, H_2O, acetone, RT, 80%; (v) 2,2-dimethoxypropane, PPTS, 96%; (vi) 2-methylbut-3-yn-2-ol, THF, Et_3N, $Pd(PPh_3)_4$, CuI, 89%; (vii) KOH, toluene, reflux, 15 h, 88%; (viii) THF, Et_3N, $Pd(PPh_3)_4$, CuI, 77–85%; (ix) *n*-BuLi, THF, $CuCl_2$, −60 °C, 15 h, 65–80%; (x) 10% HCl, CH_3OH, 25 °C, 15 h, 60–67%.

2. Results and discussion

2.1 Synthesis

5,5′-Bis(phenylethynyl)-2,2′-bithiophene based bolapolyphiles **2ET/*n*** have been synthesized *via* Kumada and Sonogashira coupling reactions as key steps, as shown in Scheme 2. Accordingly, 3-alkylthiophenes **2/*n***, obtained by the Kumada coupling of 3-bromothiophene (**1**) with appropriate *n*-alkyl magnesium bromides,[24] were iodinated in the 2-position with *N*-iodosuccinimide (NIS)[25] and then coupled with the 1,2-*O*-isopropylideneglycerol substituted phenylacetylene **9** in a Sonogashira coupling reaction,[26] leading to the 2,3-disubstituted thiophenes **10/*n***. Lithiation in the 5-position and Cu^{2+} promoted oxidative coupling[27] provided the 2,2′-dithiophenes **11/*n***. The 1,2-*O*-isopropylidene glycerol units of these compounds **11/*n*** were then deprotected to give the final compounds **2ET/*n***. The phenylacetylene building block **9** was prepared from 4-iodophenol (**4**) by allylation, *via* OsO_4-catalyzed 1,2-dihydroxylation, followed by protection of the 1,2-diol group as 1,2-*O*-isopropylidene ketal,[28] and a subsequent Sonogashira coupling with 2-methyl-3-butyn-2-ol and an alkaline deprotection of the ethynyl group.[26] The final compounds were purified by repeated crystallization from a petroleum ether : ethyl acetate ratio of 1 : 1. The detailed procedures and corresponding analysis data are collected in the ESI.† Compounds **2ET/*n*** were studied by POM, DSC, and XRD, as described in the following sections.

2.2 LC self-assembly of compounds 2ET/*n*

The phase transition temperatures and associated enthalpy values of the synthesized compounds are summarized in Table 1. Compounds **2ET/*n*** with $n = 8$, 10, and 18 exhibit enantiotropic (thermodynamically stable) LC phases whereas compound **2ET/5** with the shortest chains is non-mesomorphic, and compounds **2ET/12** and **2ET/14** with medium chain lengths display only monotropic (metastable) LC phases, which rapidly crystallize on cooling. In this homologous series, the mesophase stability, *i.e.*, the LC-Iso transition temperature, decreases with the growing chain length, and after a local minimum between $n = 12$ and 14, it slightly rises again ($n = 18$).

Between crossed polarizers, the textures of all the LC phases show birefringent, and in most cases spherulitic textures, as

Table 1 Phase types, phase transition temperatures with corresponding enthalpy values, lattice parameters, and other parameters of the bolapolyphiles **2ET/*n***[a], together with the related oligothiophenes **2T/*n***[19] and **4T/*n***[20] as reported previously[b]

Compd	T/°C [ΔH/kJ mol^{-1}]	a/nm	n_{cell}	n_{wall}	f_R
2ET/5	Cr 170[c] Iso				0.29
2ET/8	Cr < 20[d] $Col_{hex}\Delta/p6mm$ 114/111[e] [1.1] Iso	3.20	3.38	1.13	0.39
2ET/10	Cr 90 [43.5] $Col_{hex}\Delta/p6mm$ 114/112[e] [1.5] Iso	3.20	3.08	1.03	0.44
2ET/12	Cr 115 [74.9] ($Col_{hex}\Delta/p6mm$ 91[e] [1.0]) Iso	—	—	—	0.49
2ET/14	Cr 113 [59.9] ($Col_{squ}/p4mm$ 67[e] [0.8]) Iso	3.15	2.95	1.48	0.52
2ET/18	Cr 26 [20.6] $Col_{squ}/p4mm$ 73/67[e] [2.5] Iso	3.25	2.73	1.37	0.58
2T/8	Cr 56 Iso	—	—	—	0.41
2T/10	Cr 76 ($Col_{squ}/p4mm$ 71/65[d]) Iso	2.73	2.73	1.4	0.46
2T/12	Cr < 20[c] $Col_{squ}/p4mm$ 71/66[e] Iso	2.78	2.60	1.3	0.51
2T/14	Cr 50 $Col_{squ}/p4mm$ 57/46[e] Iso	2.87	2.57	1.3	0.55
2T/18	Cr 55 ($Col_{hex\text{-}6}/p6mm$ 45/34[e]) Iso	4.60	4.94	1.7	0.61
4T/5	Cr 186 (SmA^+ 152 Iso)	—	—	—	0.25
4T/8	Cr 139 $Col_{hex}\Delta/p6mm$ 171 Iso	3.74	4.13	1.4	0.35
4T/10	Cr 123 ($Col_{squ}/p4mg$ 75/68[e]) $Col_{hex}\Delta/p6mm$ 162 Iso	3.64	3.68	1.2	0.40
4T/12	Cr 138 ($Col_{squ}/p4mm$ 125 N_{cyb}135) Iso	3.52	3.69	1.8	0.44
4T/14	Cr 140 $Col_{squ}/p4mm$ 147 Iso	3.48	3.37	1.7	0.48
4T/18	Cr 100 $Col_{squ}/p4mm$ 141 Iso	3.63	3.16	1.6	0.54

[a] Determined by DSC (5 K min^{-1}, peak temperature, second scans) and confirmed by POM, for the LC-Iso phase transition, the peak temperatures from the first heating/first cooling scan are given; the values in (round) parentheses refer to monotropic phases; a = lattice parameters as determined by XRD; n_{cell} = number of molecules per unit cell, as determined from a and assuming a height of h = 0.45 nm (for details of the estimations, see Table S2 in the ESI†); n_{wall} = number of molecules arranged in the cross section of the honeycomb walls; f_R = volume fraction of the lateral alkyl chains; abbreviations of the phases: Cr = crystalline solid, Iso = isotropic liquid, $Col_{hex}\Delta/p6mm$ hexagonal columnar phase with plane group *p6mm* (triangular honeycombs), $Col_{squ}/p4mm$ = square columnar phase with plane group *p4mm* (square honeycombs), $Col_{hex\text{-}6}/p6mm$ hexagonal columnar phase representing a hexagonal honeycomb. [b] For the reference compounds only data of *p6mm* and *p4mm* phases for one selected temperature are given, for more details, see ref. 19 and 20. [c] Temperature determined by POM. [d] No crystallization was observed even after storage for several weeks. [e] Phase transition temperature on cooling.

typical for LC phases with 2D periodicity (columnar phases; see Fig. 1a and e and S1†). All these columnar phases are uniaxial, as indicated by the presence of optically isotropic homeotropic regions, where the direction of the cylinder long axis is perpendicular to the substrate surfaces (the dark areas in Fig. 1a and e and S1†). This means that the investigated columnar phases could either have a hexagonal or a square 2D lattice. Investigation with an additional λ retarder plate shows that all the columnar phases are optically negative, *i.e.*, they have a high index optical axis, which is known to be parallel to the long axis of the π-conjugated cores, perpendicular to the column long axis (see Fig. 1b and f). This is in line with polygonal honeycomb structures, in which the π-conjugated rod-like cores are arranged on an average perpendicular to the cylinder long axis.

The XRD patterns of compounds **2ET/*n*** (n = 8, 10, 14, and 18) show diffuse wide-angle scatterings with the maxima around 0.44–0.46 nm, confirming that they form true LC phases (see Fig. 1c and g and S5–S8†). Indexing of the SAXS patterns led to the phase assignments with the plane groups, as shown in Table 1. For the compounds **2ET/8** and **2ET/10**, the ratio of the reciprocal small-angle X-ray spacings is 1 : 2. A simple lamellar organization can be excluded based on the typical textures, which indicate optically negative and uniaxial columnar phases (Fig. 1a and S1a†). Thus, the small angle reflexes of the diffraction patterns were indexed as 10 and 20 reflections of hexagonal lattices with a_{hex} = 3.20 nm. These values are in the range of the molecular length (L_{mol} = 3.10–3.35 nm); L_{mol} = 3.35 nm being the largest possible length in the most stretched conformation and measured between the ends of the primary hydroxyl groups at both ends of the rod-like core (see Fig. 2). The same coincidence of L_{mol} and a_{hex} was previously observed for the $Col_{hex}\Delta/p6mm$ phases of the related compounds **4T/*n*** (n = 8, 10, see Table 1).[20] Presently, there are three known types of LC honeycombs with hexagonal symmetry formed by X-shaped bolapolyphilic (triphilic) molecules, with different relations between the hexagonal lattice parameter a_{hex} and the molecular length between the ends of the terminal polar groups (L_{mol}). These are the triangular honeycomb, where $a_{hex} = L_{mol}$,[7,18–21] the hexagon tiling[4] with $a_{hex} = 3^{1/2} L_{mol}$, and the Kagome pattern, combining hexagonal and triangular cells and having a ratio $a_{hex} = 2 L_{mol}$.[11b] The latter is only formed by molecules with two different and incompatible lateral chains as well as honeycomb super lattices combining honeycomb cells with different contents (see Fig. S3†).[11c,d] A regular rhomb tiling with the relation $a_{hex} = 3^{1/2} L_{mol}$, the same as for the hexagon tiling, has not yet been found. The coincidence of L_{mol} and a_{hex} is unique for tiling by equilateral triangles in the $Col_{hex}\Delta/p6mm$ phase, as previously observed for the related compounds **4T/*n*** (n = 8, 10, see Table 1).[29] The number of molecules organized around the triangular cells can deviate from being exactly three, because in the LC state, the individual molecules do not have fixed positions, thus this number does not even necessarily have to be an integer number, but instead represents a time and space averaged value. Each of the three walls enclosing a triangular

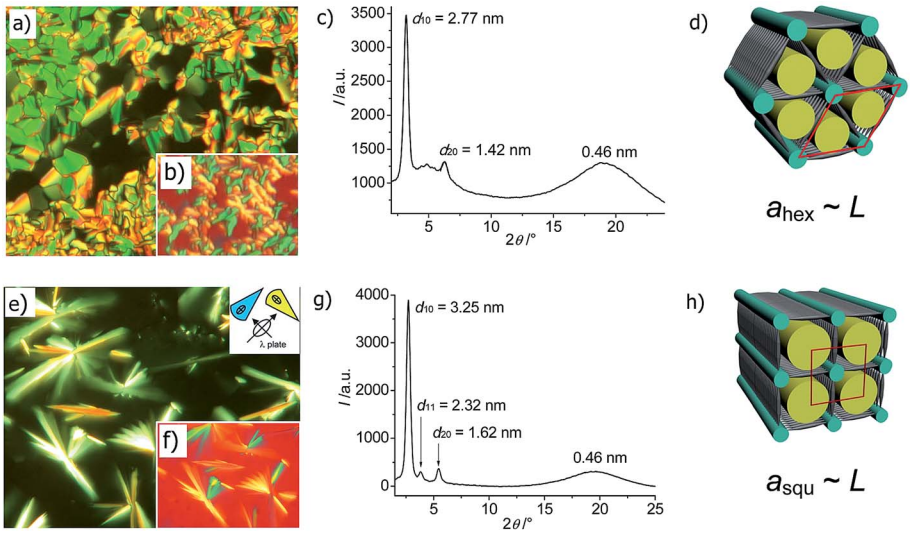

Fig. 1 Mesophases of compounds **2ET/*n***: (a) texture (crossed polarizers, $T = 80$ °C); (b) texture with λ retarder plate; (c) XRD pattern ($T = 100$ °C) and (d) model of the $Col_{hex}\Delta/p6mm$ phase of compound **2ET/10**; (e) texture ($T = 60$ °C); (f) texture with λ retarder plate; (g) XRD pattern ($T = 25$ °C) and (h) model of the $Col_{squ}/p4mm$ phase of compound **2ET/18**. The indicatrix-orientation of the λ-plate is shown in the inset in (e). The diffuse scattering in the small angle region of the XRD pattern of compound **2ET/10** is also observed at $T = 25$ °C (see Fig. S6†) and for the $Col_{hex}\Delta/p6mm$ phase of **2ET/8** (Fig. S5†), and, therefore, it is likely be due to a defective structure of the triangular honeycombs, effectively representing rhombic cells which are randomly distributed along the tree main axes of the hexagonal lattice, as previously suggested for the Col_{hex} phases of compounds **4T/*n***;[20] hence, the model (d) shows a simplified and idealized picture neglecting these defects.

honeycomb cell should be at least one aromatic core in (lateral) diameter, but occasionally also two molecules (or even three) can be organized either side-by-side or in a staggered mode. The resulting average number of molecules organized laterally in each of the honeycomb walls (n_{wall}) is estimated by dividing the unit cell volume (assuming a stratum with a height of 0.45 nm, approximately corresponding to the average diameter of the rotationally disordered aromatic cores and corresponding to the maximum of the wide angle scattering in XRD) by the molecular volume (estimated using tabulated crystal volume increments,[30] as described in Table S2†), and then divided by the number of walls per unit cell, *i.e.*, by three for the triangular and the hexagon tiling and by two for the square tiling. The estimated number of molecules arranged laterally side by side in the cross section of the honeycomb walls (n_{wall}) is between 1.0 and 1.1 for the triangular honeycombs of compounds **2ET8–2ET12** (see Table 1 and S2†), in line with the honeycomb walls formed by (on average) a single molecule in the cross section.

As the available space within the triangular honeycomb cells is restricted, a frustration arises from the overcrowding of the honeycomb cells as the chain length grows further. Therefore, the LC phase stability decreases at the transition from **2ET/10** ($T_{Iso\text{-}LC}$ = 112 °C) to **2ET/12** ($T_{Iso\text{-}LC}$ = 91 °C, see Table 1). Compounds **2ET/12** and **2ET/14**, with medium lateral chain lengths, show LC phases only on cooling (monotropic phases, see Fig. S2c and S2d†). Because of rapid crystallization during the exposure time of the XRD measurement, confirmation of the LC phase structure of compound **2ET/12** was not possible in this way. However, investigations of the binary mixtures provided evidence that the columnar phase of **2ET/12** is a hexagonal columnar phase with a triangular honeycomb structure, just like that of **2ET/10**. This was indicated by the continuous growth of the spherulitic texture of the $Col_{hex}\Delta/p6mm$ phase of compound **2ET/10** into the region of **2ET/12** without any intermediate minimum, maximum, or visible miscibility gap (see Fig. 3a and S4†). In contrast, in the contact region between the LC phases of compounds **2ET/12** and **2ET/14**, in a certain concentration range, there is an isotropic liquid ribbon separating them (see Fig. 3b), indicating that the two LC phases should have a different structure and, thus, **2ET/14** cannot form a triangular honeycomb. Because the aromatic core length of the **2ET/*n*** compounds is exactly the same, there is a matching in the honeycomb wall dimensions of the different compounds, and therefore their honeycomb frames are compatible with each other. For this reason, honeycombs with identical polygon shapes have complete miscibility whereas those with different polygon shape cannot mix, and this allows

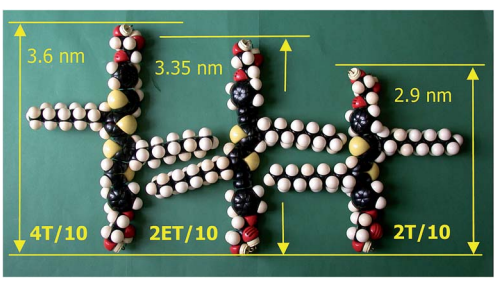

Fig. 2 CPK models and estimated molecular lengths (L_{mol}) of compounds **2ET/*n*** and the related compounds **2T/*n*** and **4T/*n*** ($n = 10$), shown in their most extended conformation.

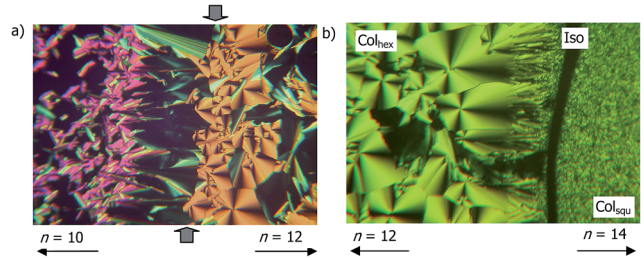

Fig. 3 (a) Contact region between the triangular honeycomb type LC phases of **2ET/10** and **2ET/12** at $T = 84$ °C, the arrows indicate the approximate position of the boundary between the two compounds; the dark areas represent the homeotropically aligned regions of the Col$_{hex}$Δ/*p6mm* phases; the development of the contact region is shown in Fig. S3;† the reduced birefringence of **2ET/12** compared to **2ET/10** (purple *vs.* orange) is assumed to be due to the decreased orientational order parameter of the aromatic cores in the honeycomb walls, resulting from the overcrowding of the honeycomb cells by the alkyl chains, occurring before the transition to the square honeycomb structure. The cores are more strictly parallel to the column normal in the Col$_{hex}$ phase of **2ET/10** whereas for **2ET/12** there is a reduced order parameter of these cores, due to the increased average deviation from being exactly parallel to the column normal. (b) Contact region between the triangular honeycomb of **2ET/12** and the square honeycomb of **2ET/14** at $T = 61$ °C; the isotropic ribbon is an isotropic liquid region observed down to $T \sim 60$ °C, indicating the incompatibility of the two columnar phases with different symmetries.

the use of miscibility studies for LC phase assignment of these compounds.

Indeed, XRD investigations confirm a square columnar phase with the *p4mm* plane group symmetry for **2ET/14** (Col$_{squ}$/*p4mm*), as evident from the ratio of the reciprocal spacing $1 : 2^{1/2} : 2$ in the small angle scatterings in the XRD pattern (see Fig. S7 and Table S1†). The lattice parameter ($a_{squ} = 3.15$ nm) is in the range of the molecular length ($L_{mol} = 3.10$–3.35 nm), which is in line with a square honeycomb structure for this uniaxial and optical negative mesophase. The same *p4mm* phase was found for compound **2ET/18** with the longest chains (see Fig. 1g and S8 and Table S1†). Fig. 1h shows the proposed arrangement of the molecules **2ET/*n*** ($n = 14$, 18) in the Col$_{squ}$/*p4mm* phases, where rod-like cores are fused together *via* hydrogen bonding located at both ends and leads to them forming honeycombs with a square cross sectional area around the lipophilic columns incorporating the lateral alkyl chains. The average number of molecules in the honeycomb walls is $n_{wall} \sim 1.4$–1.5, which agrees well with the values observed previously for the square honeycomb LC phases formed by related compounds (see Table 1).[18–20]

A remarkable feature in the XRD patterns of all the Col$_{hex}$Δ/*p6mm* phases is the presence of an additional diffuse small angle scattering. This is reproducibly observed, independent of temperature (see Fig. S6† for the diffraction pattern of the supercooled sample of **2ET/10** at $T = 25$ °C), such that it cannot be an artifact, due to its coexistence with an isotropic liquid phase as a result of decomposition or for any other reason. This kind of diffraction pattern was previously observed for the Col$_{hex}$Δ/*p6mm* phases of the related compounds **4/*n*** ($n = 8$, 10, see Table 1) and interpreted as indication of a defective structure of the triangular honeycombs, actually formed by rhombic cylinder segments with a time and space averaged random orientation of the rhomb's long axis along the three directions of a hexagonal lattice.[20,31] This model is in line with the reduced average number of molecules arranged laterally side by side in the cross-section of the honeycomb walls (n_{wall}) being only 1.1 to 1.0 for compounds **2ET/10** and **2ET/12**, respectively. Typically, values between 1.3 and 1.8 were observed for the other honeycomb phases of X-shaped bolapolyphiles (see Table 1).[11] Thus, besides staggering and a lateral side-by-side packing, which shift the n_{wall} to larger values, there should also be hole-defects in the walls, shifting the n_{wall} to smaller average values. In addition, the decreasing birefringence of the Col$_{hex}$Δ/*p6mm* phase upon approaching the limits of its existence range (see contact region between **2ET/10** and **2ET/12** in Fig. 3a) indicates a decreasing order parameter of the π-conjugated cores in the honeycomb walls (larger deviations form an alignment perpendicular to the column long axis), which is in line with the proposed defective structure of these trigonal honeycombs. With growing alkyl chain length, the hole formation becomes more influential, and leads to an increasing disorder of the aromatic cores, and hence the birefringence and the stability of the Col$_{hex}$ phase decrease. Below a critical value of $n_{wall} \sim 1.0$, the triangular honeycombs become unstable, giving way to a square honeycomb at the transition of the alkyl chain length from $n = 12$ to $n = 14$. The square honeycombs then have an increased perfection, as indicated by the complete absence of any diffuse small angle scattering in the XRD patterns (see Fig. S7†).

2.3 Comparison of different series of 2,2′-bithiophene based bolapolyphiles

A comparison of the three series of compounds with distinct molecular lengths, namely **2T/*n*** ($L_{mol} = 2.9$ nm), **2ET/*n*** ($L_{mol} = 3.35$ nm), and **4T/*n*** ($L_{mol} = 3.6$ nm; all measured in the same stretched conformation, see Fig. 2), provides additional insights. All three series have similar phase sequences, where, depending on the structure, the distinct phases are shifted towards longer or shorter alkyl chain lengths. The dithiophenes **2T/*n*** have the lowest phase transition temperatures, which increase in the sequence **2T/*n*–2ET/*n*–4T/*n*** with the growing length of the rod-like core. This indicates that increasing the core length stabilizes the honeycombs. A major contribution to the LC phase stability might arise from the growing incompatibility of the longer rigid rods with the flexible alkyl chains, thus enhancing the phase stability by increasing nano-segregation mainly due to the entropy driven rigid-flexible incompatibility. In the same order, **2T/*n*–2ET/*n*–4T/*n***, there is also a tendency towards higher melting temperatures, though there are exceptions.

The compounds of series **2T/*n*** show predominantly square honeycomb phases (Col$_{squ}$/*p4mm*). Here, the relatively short core unit provides only limited space inside the honeycomb cells and, therefore, for the chain length $n = 10$–14, only square cells can provide sufficient space. Only for compound **2T/18** with the longest chains ($n = 18$), is a Col$_{hex}$/*p6mm* phase formed,

but in this case it is not a triangular honeycomb phase, but instead a LC honeycomb formed by hexagonal cells with six molecules in the circumference of the cells ($Col_{hex\text{-}6}/p6mm$). Compound **2T/8** with shorter octyl chains does not form any LC phase. So overall, triangular LC honeycombs seem to be unstable for these compounds with relatively short rod-like cores. For compounds **2ET/*n*** with a longer aromatic core, reported herein, additional space is available in the honeycomb cells and therefore there is a tendency to form smaller triangular honeycomb cells if the alkyl chain length is $n = 8$–12. Hence, besides the square honeycombs, also triangular honeycombs were observed ($Col_{hex}\Delta/p6mm$). On chain elongation, the stability of the triangular honeycomb is reduced and after a local minimum between $n = 12$ and 14, further chain elongation leads to square honeycomb phases for $n = 14$–18. For the series of compounds **4T/*n*** with the longest aromatic cores, an even broader variety of LC phases was found, in this case ranging from SmA *via* $Col_{hex}\Delta/p6mm$, $Col_{squ}/p4gm$, a nematic phase (N), to $Col_{squ}/p4mm$. In this series of compounds, too, there is a local minimum for the mesophase stability, depending on alkyl chain length. This minimum, which is associated with a transition from triangular ($p6mm$) to square honeycombs ($p4mm$), is shifted for compounds **4T/*n*** a bit to shorter chain lengths, compared to the series **2ET/*n*** ($n = 12$–14 for **2ET/*n*** and $n = 12$ for **4T/*n***; even for $n = 12$ there is a low temperature $p4gm$ honeycomb phase comprising squares). This is surprising, because the longer core of **4T/*n*** should provide more free space in the honeycomb cells and thus should favor the formation of triangular honeycombs more strongly than **2ET/*n***, *i.e.*, it would be expected that the minimum should be shifted in the opposite direction. That this is not the case can be explained by the smaller average cross section of the aromatic cores involving the slim C–C triple bond compared to the more bulky thiophene ring of **4T/*n***. Thus, for compounds **2ET/*n***, more space remains available in the honeycomb cells to be filled by the alkyl chains, and therefore longer chains are required to fill the square honeycombs. On the other hand, the longer rod-like core of **4T/*n*** give rise to an increased tendency for parallel alignment of the cores and, therefore, SmA and nematic phases were observed for compounds **4T/*n***, which are missing for the series **2T/*n*** and **2ET/*n*** with shorter cores (Table 1). In addition, in the case of **2ET/*n***, the linear acetylene units at the 2,2′-dithiophene core provide a more pronounced zigzag like overall molecular shape (see Fig. 2), which might additionally contribute to the reduced tendency for the orientational order of these cores. Besides these main effects, there could be additional structural effects influencing the mode of self-assembly, such as the rotational barriers between the individual rings forming the rigid core, which should be very different for compounds **2ET/*n*** and **4T/*n***, leading to distinct conformations and overall flexibilities of the core units. Moreover, the conformational freedom of the alkyl chains should be affected by the type of adjacent unit in the 5- and 5′-positions of the 2,2′-dithiophene core and this might affect the mode of chain packing inside the honeycomb cells.

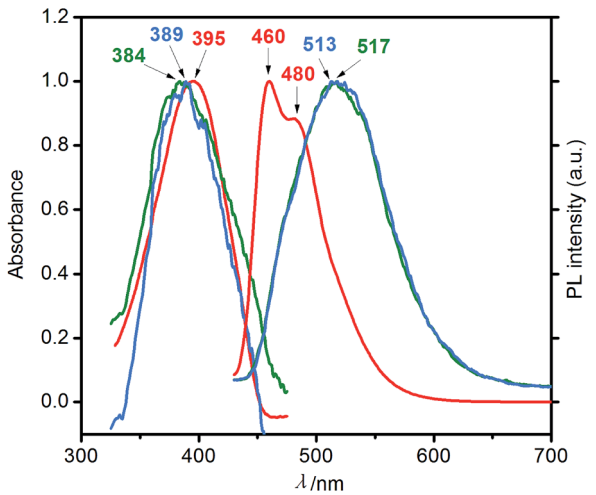

Fig. 4 UV-vis absorption spectra (left) and photoluminescence spectra (right) of compound **2ET/18** in $CHCl_3$ solution (10^{-6} M) (red line), in a liquid crystalline state at 35 °C (green line), and in a solid thin film (blue line).

2.4 Luminescent properties

The UV-vis absorption and fluorescence spectroscopic data in $CHCl_3$ solution ($c = 10^{-6}$ mol L^{-1}) and in the condensed states are shown in Fig. 4 for compound **2ET/18**, which was chosen to be investigated. This compound shows the maximum absorption peaks at 395 nm, 384 nm, and 389 nm in solution, in the LC state, and in the solid state, respectively, which may be attributed to the π–π* transitions. The blue shifts (of about 11 nm in the LC state and 6 nm in the solid state, respectively) suggest the formation of π-stacked aggregates with a H-type parallel stacking mode, both in LC state and in the solid state.[32] The photoluminescence (PL) spectrum of **2ET/18** in the LC phase and in the solid state exhibits a broad and red-shifted emission with maxima at 517 nm and 513 nm, respectively, while the solution displays a structured emission with maxima at 460 nm and 480 nm. Hence, the Stokes shift has a remarkably large value of 124–133 nm in the condensed states (*i.e.*, the LC state and solid state) related to 65 nm in $CHCl_3$ solution, which confirms the strong intramolecular charge transfer in compound **2ET/18**.[33] This feature indicates that these compounds have a significant potential for application in fluorescence sensors[34] and photoactive functional assemblies.[35]

3. Conclusion

In summary, a series of novel X-shaped bolapolyphiles incorporating a rigid and fluorescence active 5,5′-bis(phenylethynyl)-2,2′-bithiophene core with glycerol groups at both ends and two lateral alkyl chains was synthesized through a straightforward synthesis pathway. By elongation of the lateral alkyl chains, a transition from defective triangular to square honeycomb LCs, separated by a local minimum of the LC phase stability was observed. This indicates that the additional triple bonds, though enabling the formation of triangular honeycombs, obviously do not provide that degree of core elongation as would be required for the occurrence of additional intermediate

phases combining triangular and square cells in a common superstructure, which would be required to give rise to larger superlattice structures, and eventually leading to quasi-periodic columnar LC phases.

4. Experimental

^{1}H NMR and ^{13}C NMR spectra were recorded in $CDCl_3$ solution on a Bruker-DRX-500 spectrometer with tetramethylsilane (TMS) as the internal standard. Elemental analysis was performed using an Elementar VARIO EL elemental analyzer. A Mettler heating stage (FP 82 HT) was used for the polarizing optical microscopy (POM, Optiphot 2, Nikon), and DSCs were recorded with a DSC-7 calorimeter (PerkinElmer) at 10 K min^{-1}. X-Ray diffraction (XRD) of the surface aligned samples was performed using a 2D-detector (HI-Star, Siemens or Vantec-500, Bruker). Ni filtered and pin hole collimated CuKα was used. Details of the synthesis and purification, and the analytical data are reported in the ESI.†

Acknowledgements

This work was supported by the National Natural Science Foundation of China [no. 21364017, no. 21274119], the Yunnan Natural Science Foundation [no. 2013FA007] and Scholarship Award for Excellent Doctoral Student of Yunnan Province and foundation [no. ynuy201418]. M.P. and C.T. acknowledge the support by DFG (FOR 1145).

References

1 (*a*) C.-A. Palma, M. Cecchioni and P. Samoni, *Chem. Soc. Rev.*, 2012, **41**, 3713–3730; (*b*) J. M. Lehn, *Angew. Chem., Int. Ed.*, 2013, **52**, 2836–2850; (*c*) S. I. Stupp and L. C. Palmer, *Chem. Mater.*, 2014, **26**, 507–518.

2 (*a*) H. Li, M. Eddaoudi, M. O'Keeffe and O. M. Yaghi, *Nature*, 1999, **402**, 276–279; (*b*) O. M. Yaghi, M. O'Keeffe, N. W. Ockwig, H. K. Chae, M. Eddaoudi and J. Kim, *Nature*, 2003, **423**, 705–714; (*c*) A. P. Cote, A. I. Benin, N. W. Ockwig, M. O'Keeffe, A. J. Matzger and O. M. Yaghi, *Science*, 2005, **310**, 1166–1170; (*d*) X. Feng, X. Ding and D. Jiang, *Chem. Soc. Rev.*, 2012, **41**, 6010–6022.

3 (*a*) S. Wan, J. Guo, J. Kim, H. Ihee and D. Jiang, *Angew. Chem.*, 2008, **120**, 8958–8962; (*b*) E. L. Spitler, J. W. Colson, F. J. Uribe-Romo, A. R. Woll, M. R. Giovino, A. Saldivar and W. R. Dichtel, *Angew. Chem., Int. Ed.*, 2012, **51**, 2623–2627; (*c*) X. Feng, L. Chen, Y. Honso, O. Saengsawang, L. Liu, L. Wang, A. Saeki, S. Irle, S. Seki, Y. Dong and D. Jiang, *Adv. Mater.*, 2012, **24**, 3026–3031; (*d*) M. E. Foster, J. D. Azoulay, B. M. Wong and M. D. Allendorf, *Chem. Sci.*, 2014, **5**, 2081–2090.

4 (*a*) M. Kölbel, T. Beyersdorff, X. H. Cheng, C. Tschierske, J. Kain and S. Diele, *J. Am. Chem. Soc.*, 2001, **123**, 6809–6818; (*b*) X. H. Cheng, M. Prehm, M. K. Das, J. Kain, U. Baumeister, S. Diele, D. Leine, A. Blume and C. Tschierske, *J. Am. Chem. Soc.*, 2003, **125**, 10977–10996; (*c*) M. Prehm, F. Liu, U. Baumeister, X. Zeng, G. Ungar and C. Tschierske, *Angew. Chem., Int. Ed.*, 2007, **46**, 7972–7975; (*d*) M. Prehm, C. Enders, M. Y. Anzahaee, B. Glettner, U. Baumeister and C. Tschierske, *Chem.–Eur. J.*, 2008, **14**, 6352–6368.

5 (*a*) C. Tschierske, *Chem. Soc. Rev.*, 2007, **36**, 1930–1970; (*b*) C. Tschierske, C. Nürnberger, H. Ebert, B. Glettner, M. Prehm, F. Liu, X. B. Zeng and G. Ungar, *Interface Focus*, 2011, **2**, 669–680; (*c*) G. Ungar, C. Tschierske, V. Abetz, R. Holyst, M. A. Bates, F. Liu, M. Prehm, R. Kieffer, X. B. Zeng, M. Walker, B. Glettner and A. Zywocinski, *Adv. Funct. Mater.*, 2011, **21**, 1296–1323.

6 C. Tschierske, *Angew. Chem., Int. Ed.*, 2013, **52**, 8828–8878.

7 F. Liu, B. Chen, U. Baumeister, X. B. Zeng, G. Ungar and C. Tschierske, *J. Am. Chem. Soc.*, 2007, **129**, 9578–9579.

8 Q. Zhou, T. Chen, J. Zhang, L. Wan, P. Xie, C. C. Han, S. Yan and R. Zhang, *Tetrahedron Lett.*, 2008, **49**, 5522–5526.

9 J. W. Goodby, J. P. Collings, T. Kato, C. Tschierske, H. F. Gleeson and P. Raynes, *Handbook of Liquid Crystals*, Wiley-VCH, Weinheim, Germany, 2nd edn, 2014.

10 Besides these low molecular mass LC molecules involving a rigid segment, tilings related to the LC honeycombs were also observed for mictoarm triblock star copolymers,[5c] see: S. Sioula, N. Hadjichristidis and E. L. Thomas, *Macromolecules*, 1998, **31**, 8429–8432; Y. Matsushita, K. Hayashida and A. Takano, *Macromol. Rapid Commun.*, 2010, **31**, 1579–1587, and more recently for lyotropic systems of triblock star molecules involving fluorocarbon, hydrocarbon and oligo(ethylene oxide) chains: L. de Campo, T. Varslot, M. J. Moghaddam, J. J. K. Kirkensgaard, K. Mortensen and S. T. Hyde, *Phys. Chem. Chem. Phys.*, 2011, **13**, 3139–3152.

11 (*a*) R. Kieffer, M. Prehm, B. Glettner, K. Pelz, U. Baumeister, F. Liu, X. B. Zeng, G. Ungar and C. Tschierske, *Chem. Commun.*, 2008, 3861–3863; (*b*) B. Glettner, F. Liu, X. B. Zeng, M. Prehm, U. Baumeister, M. A. Bates, M. Walker, P. Boesecke, G. Ungar and C. Tschierske, *Angew. Chem., Int. Ed.*, **47**, 9063–9066; (*c*) X. B. Zeng, R. Kieffer, B. Glettner, C. Nürnberger, F. Liu, K. Pelz, M. Prehm, U. Baumeister, H. Hahn, H. Lang, G. A. Gehring, C. H. M. Weber, J. K. Hobbs, C. Tschierske and G. Ungar, *Science*, 2011, **331**, 1302–1306; (*d*) F. Liu, R. Kieffer, X.-B. Zeng, K. Pelz, M. Prehm, G. Ungar and C. Tschierske, *Nat. Commun.*, 2012, **3**, 1104–1110.

12 Bolaamphiphiles represent molecules composed of a lipophilic core and hydrophilic groups at each end see: J.-H. Fuhrhop and T. Yang, *Chem. Rev.*, 2004, **104**, 2901–2937; bolapolyphiles have one (T-shaped bolapolyphiles) or more additional lateral chain(s) at this core (*e.g.* X-shaped bolapolyphiles), which are incompatible with the core and the polar end groups.[5] For molecules with two lateral chains, the chains could be similar and miscible (bolatriphiles)[11a] or very different and immiscible (bolatetraphiles).[11b–d]

13 (*a*) A. J. Crane, F. J. Martinez-Veracoechea, F. A. Escobedo and E. A. Mueller, *Soft Matter*, 2008, **4**, 1820–1829; (*b*) M. Bates and M. Walker, *Soft Matter*, 2009, **5**, 346–353; (*c*)

T. D. Nguyen and S. C. Glotzer, *ACS Nano*, 2010, **4**, 2585–2594.
14 B. Chen, X. Zeng, U. Baumeister, G. Ungar and C. Tschierske, *Science*, 2005, **307**, 96–99.
15 (*a*) M. Oxborrow and C. L. Henley, *Phys. Rev. B: Condens. Matter*, 1993, **48**, 6966–6998; (*b*) M. O'Keeffe and M. M. J. Treacy, *Acta Crystallogr., Sect. A: Found. Crystallogr.*, 2009, **66**, 5–9.
16 T. Dotera, *J. Polym. Sci., Part B: Polym. Phys.*, 2012, **50**, 155–167.
17 X. H. Cheng, X. Dong, R. Huang, X. B. Zeng, G. Ungar, M. Prehm and C. Tschierske, *Chem. Mater.*, 2008, **20**, 4729–4738.
18 (*a*) M. Prehm, G. Götz, P. Bäuerle, F. Liu, G. Ungar and C. Tschierske, *Angew. Chem., Int. Ed.*, 2007, **46**, 7856–7859; (*b*) X. H. Cheng, X. Dong, G. H. Wei, M. Prehm and C. Tschierske, *Angew. Chem., Int. Ed.*, 2009, **48**, 8014–8017.
19 H. F. Gao, Y. F. Ye, L. Y. Kong, X. H. Cheng, M. Prehm, H. Ebert and C. Tschierske, *Soft Matter*, 2012, **8**, 10921–10931.
20 X. H. Cheng, H. F. Gao, X. P. Tan, X. Y. Yang, M. Prehm, H. Ebert and C. Tschierske, *Chem. Sci.*, 2013, **4**, 3317–3331.
21 W. Bu, H. F. Gao, X. P. Tan, X. Dong, X. H. Cheng, M. Prehm and C. Tschierske, *Chem. Commun.*, 2013, **49**, 1756–1758.
22 M. Funahashi, *J. Mater. Chem. C*, 2014, **2**, 7451–7459.
23 (*a*) C. Li and Y. Li, *Macromol. Chem. Phys.*, 2008, **209**, 1541–1552; (*b*) F. Silvestri and A. Marrocchi, *Int. J. Mol. Sci.*, 2010, **11**, 1471–1508; (*c*) M. Seri, A. Marrocchi, D. Bagnis, R. Ponce, A. Taticchi, T. J. Marks and A. Facchetti, *Adv. Mater.*, 2011, **23**, 3827–3831; (*d*) F. Diederich, P. J. Stang and R. R. Tykwinski, *Acetylene Chemistry: Chemistry, Biology and Materials Science*, Wiley-VCH, Weinheim, 2005.
24 (*a*) J. Pei, J. Ni, X. H. Zhou, X. Y. Cao and Y. H. Lai, *J. Org. Chem.*, 2002, **67**, 8104–8113; (*b*) R. D. McCullough, R. D. Lowe, M. Jayaraman and D. L. Anderson, *J. Org. Chem.*, 1993, **58**, 904–912; (*c*) C. V. Pham, H. B. Mark and H. Zimmer, *Synth. Commun.*, 1986, **16**, 689–696.
25 M. Melucci, G. Barbarella, M. Zambianchi, P. Di Pietro and A. Bongini, *J. Org. Chem.*, 2004, **69**, 4821–4828.
26 (*a*) J. L. Wang, J. Yan, Z. M. Tang, Q. Xiao, Y. G. Ma and J. Pei, *J. Am. Chem. Soc.*, 2008, **130**, 9952–9962; (*b*) J. L. Wang, Z. M. Tang, Q. Xiao, Q. F. Zhou, Y. G. Ma and J. Pei, *Org. Lett.*, 2008, **10**, 17–20.
27 P. Bäuerle, T. Fischer, B. Bidlingmaier, A. Stabel and J. P. Rabe, *Angew. Chem., Int. Ed.*, 1992, **34**, 303–307.
28 X. P. Tan, L. Y. Kong, H. Dai, X. H. Cheng, F. Liu and C. Tschierske, *Chem.–Eur. J.*, 2013, **19**, 16303–16313.
29 The tiling by triangular cells with different content in adjacent cells has the same ratio, but the plane group symmetry is *p*3*m*1 in this case, this tiling pattern is impossible for the compounds reported herein, as it would require the presence of two sufficiently different lateral chains that are capable of segregation into different cells.[11c]
30 A. Immirzi and B. Perini, *Acta Crystallogr., Sect. A: Cryst. Phys., Diffr., Theor. Gen. Crystallogr.*, 1977, **3**, 216–218.
31 This random rhomb tiling is distinct from the discrete hexagonal rhomb tiling on a larger hexagonal lattice (see Fig. S3,† top right) due to the switching of the rhombs orientation taking place not only between adjacent columns, but also along the individual columns.
32 T. Yasuda, K. Kishimoto and T. Kato, *Chem. Commun.*, 2006, 3399–3401.
33 J. L. Wang, Q. Xiao and J. Pei, *Org. Lett.*, 2010, **12**, 4164–4167.
34 (*a*) Z. P. Liu, C. L. Zhang, W. J. He, F. Qian, X. L. Yang, X. Gao and Z. J. Guo, *New J. Chem.*, 2010, **34**, 656–660; (*b*) S. Yao, K. J. Schafer-Hales and K. D. Belfield, *Org. Lett.*, 2007, **9**, 5645–5648.
35 Q. Yan, Z. Luo, K. Cai, Y. Ma and D. Zhao, *Chem. Soc. Rev.*, 2014, **43**, 4199–4221.